

Intrinsically Chiral Paddlewheel Diruthenium Complexes

Isabel Coloma,^a Santiago Herrero,^{a,b} and Miguel Cortijo^{*a}

^aMatMoPol Research Group, Inorganic Chemistry Department, Faculty of Chemical Sciences, Complutense University of Madrid, E-28040 Madrid, Spain.

^bKnowledge Technology Institute, Complutense University of Madrid, Campus de Somosaguas, E-28223 Pozuelo de Alarcón, Madrid, Spain.

Correspondence: miguelcortijomontes@ucm.es

INDEX

S1. Mass spectrometry

- Figure S1. Mass spectrum of *cis*-[Ru₂Cl(μ-DPhF)₂(μ-OAc)₂] and enlargement of the base peak and the calculated isotopic pattern (DPhF = *N,N'*-diphenylformamidinate).
- Figure S2. Mass spectrum of *cis*-[Ru₂Cl(μ-DAniF)₂(μ-OAc)₂] and enlargement of the base peak and the calculated isotopic pattern (DAniF = *N,N'*-bis(*p*-methoxyphenyl)formamidinate).
- Figure S3. Mass spectrum of *cis*-[Ru₂Cl(μ-DPhF)₂(μ-hmp)(μ-OAc)] (**Ruhmp**) and enlargement of the base peak and the calculated isotopic pattern.
- Figure S4. Mass spectrum of *cis*-[Ru₂Cl(μ-DPhF)₂(μ-amp)(μ-OAc)] (**Ruamp**) and enlargement of the base peak and the calculated isotopic pattern.
- Figure S5. Mass spectrum of *cis*-[Ru₂Cl(μ-DAniF)₂(μ-hmp)(μ-OAc)] (**Ru'hmp**) and enlargement of the base peak and the calculated isotopic pattern.
- Figure S6. Mass spectrum of *cis*-[Ru₂Cl(μ-DAniF)₂(μ-amp)(μ-OAc)] (**Ru'amp**) and enlargement of the base peak and the calculated isotopic pattern.

S2. Infrared spectroscopy

- Figure S7. Infrared spectra of **Ruhmp**, **Ruamp**, **Ru'hmp** and **Ru'amp**.
- Figure S8. Comparison between the IR spectra of *cis*-[Ru₂Cl(μ-DAniF)₂(μ-OAc)₂], **Ru'hmp** and **Ru'amp**.
- Figure S9. Comparison between the IR spectra of **Ruhmp** and **Ruamp**.
- Figure S10. Comparison between the IR spectra of **Ruhmp** and **Ru'hmp**.

S3. Single crystal X-ray diffraction

- Table S1. Crystal and structure refinement data for **Ruhmp**.
- Table S2. Crystal and structure refinement data for **Ruamp**·Et₂O.
- Table S3. Crystal and structure refinement data for **Ru'hmp**.
- Table S4. Crystal and structure refinement data for **Ru'amp**·0.5C₆H₁₂.

S4. Magnetic measurements

- Figure S11. Temperature dependence of the molar susceptibility χ_M and $\chi_M T$ for **Ruhmp**.
- Figure S12. Temperature dependence of the molar susceptibility χ_M and $\chi_M T$ for **Ruamp**.
- Figure S14. Temperature dependence of the molar susceptibility χ_M and $\chi_M T$ for **Ru'amp**.
- Equations S1-S4 employed in the fitting of the magnetic data

S5. Procedure employed to assign polyhedral symbol, coordination index, configuration number and chirality symbol to coordination compounds with paddlewheel structure

S1. Mass spectrometry

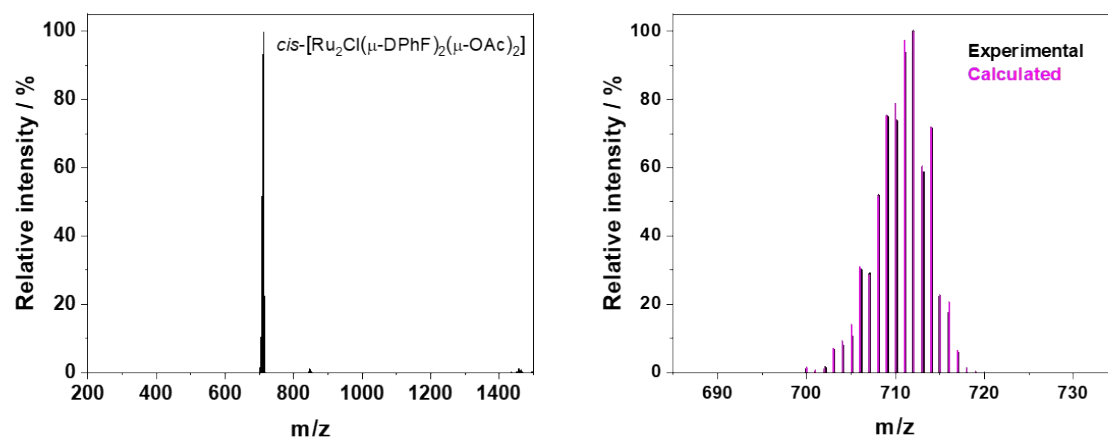


Figure S1. Mass spectrum (ESI⁺) of $cis\text{-}[\text{Ru}_2\text{Cl}(\mu\text{-DPhF})_2(\mu\text{-OAc})_2]$ (left) and enlargement of the $[\text{M}-\text{Cl}]^+$ base peak (black) and the calculated isotopic pattern (pink) (right).

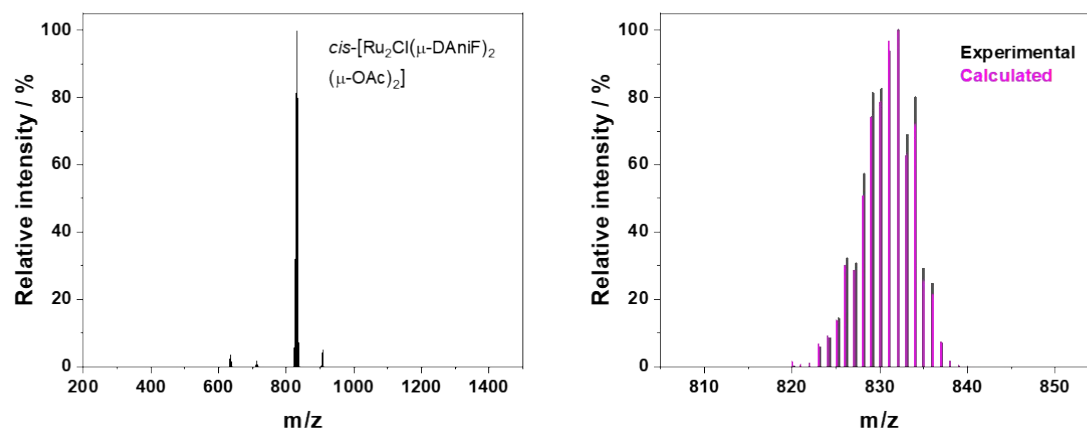


Figure S2. Mass spectrum (ESI⁺) of $cis\text{-}[\text{Ru}_2\text{Cl}(\mu\text{-DAniF})_2(\mu\text{-OAc})_2]$ (left) and enlargement of the $[\text{M}-\text{Cl}]^+$ base peak (black) and the calculated isotopic pattern (pink) (right).

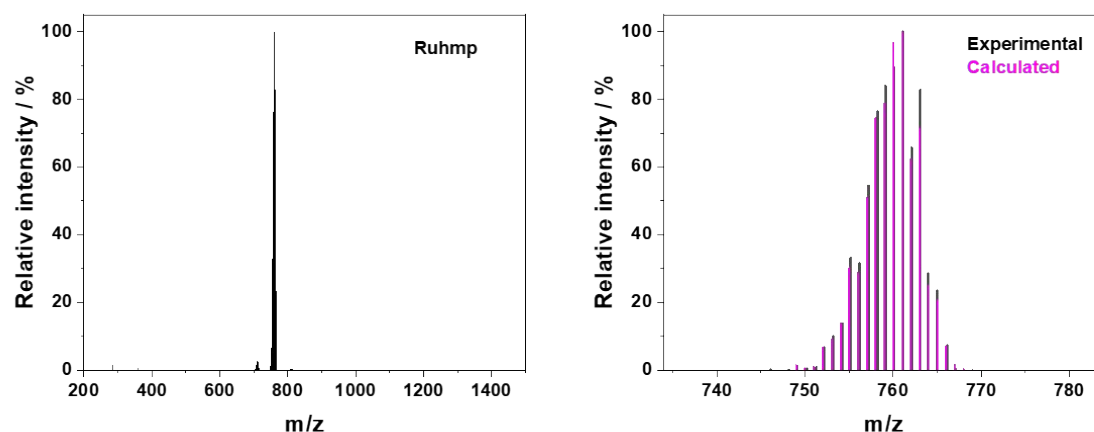


Figure S3. Mass spectrum (ESI⁺) of **Ruhmp** (left) and enlargement of the $[\text{M}-\text{Cl}]^+$ base peak (black) and the calculated isotopic pattern (pink) (right).

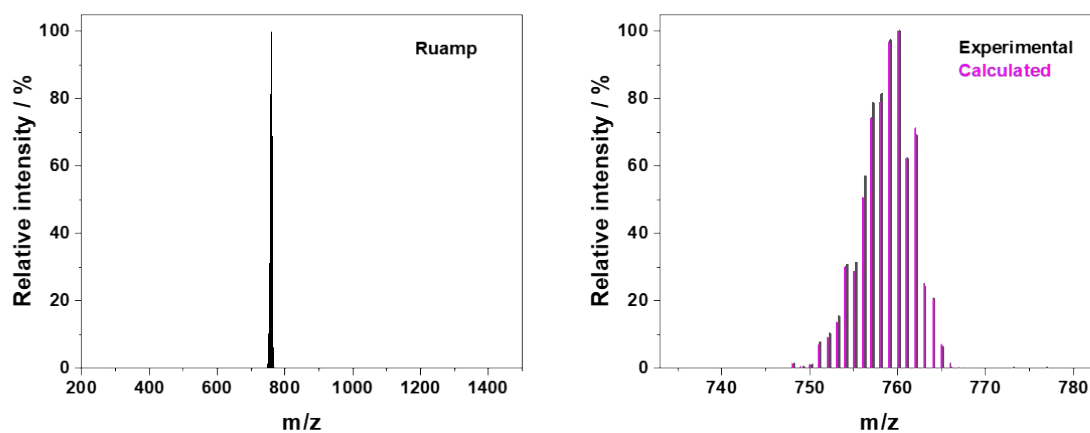


Figure S4. Mass spectrum (ESI⁺) of **Ruamp** (left) and enlargement of the [M-Cl]⁺ base peak (black) and the calculated isotopic pattern (pink) (right).

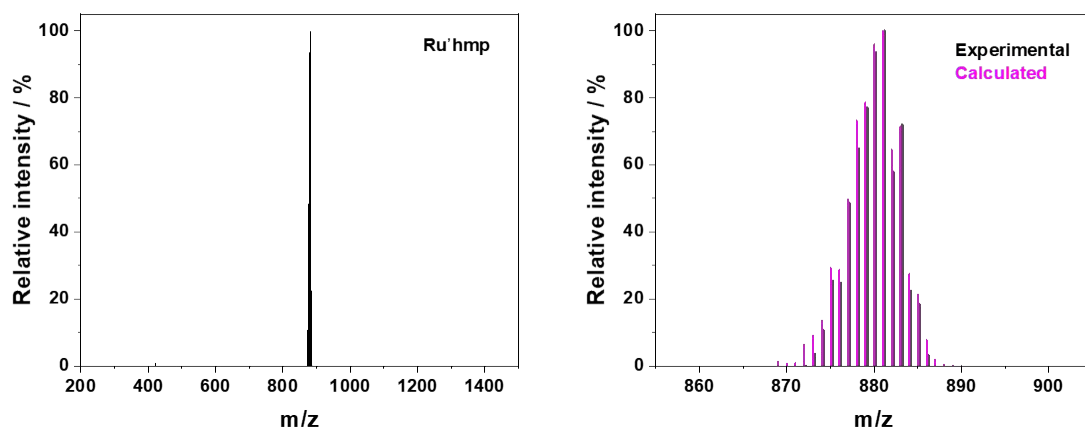


Figure S5. Mass spectrum (ESI⁺) of **Ru'hmp** (left) and enlargement of the [M-Cl]⁺ base peak (black) and the calculated isotopic pattern (pink) (right).

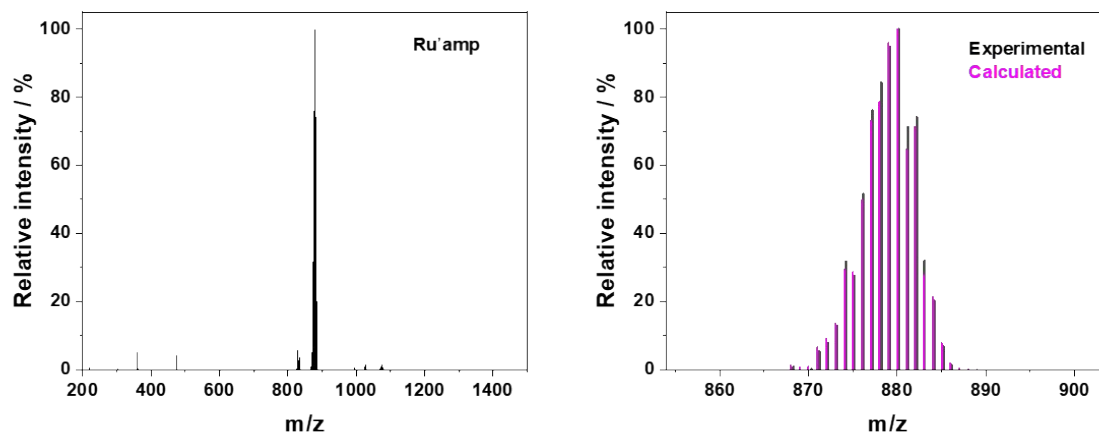


Figure S6. Mass spectrum (ESI⁺) of **Ru'amp** (left) and enlargement of the [M-Cl]⁺ base peak (black) and the calculated isotopic pattern (pink) (right).

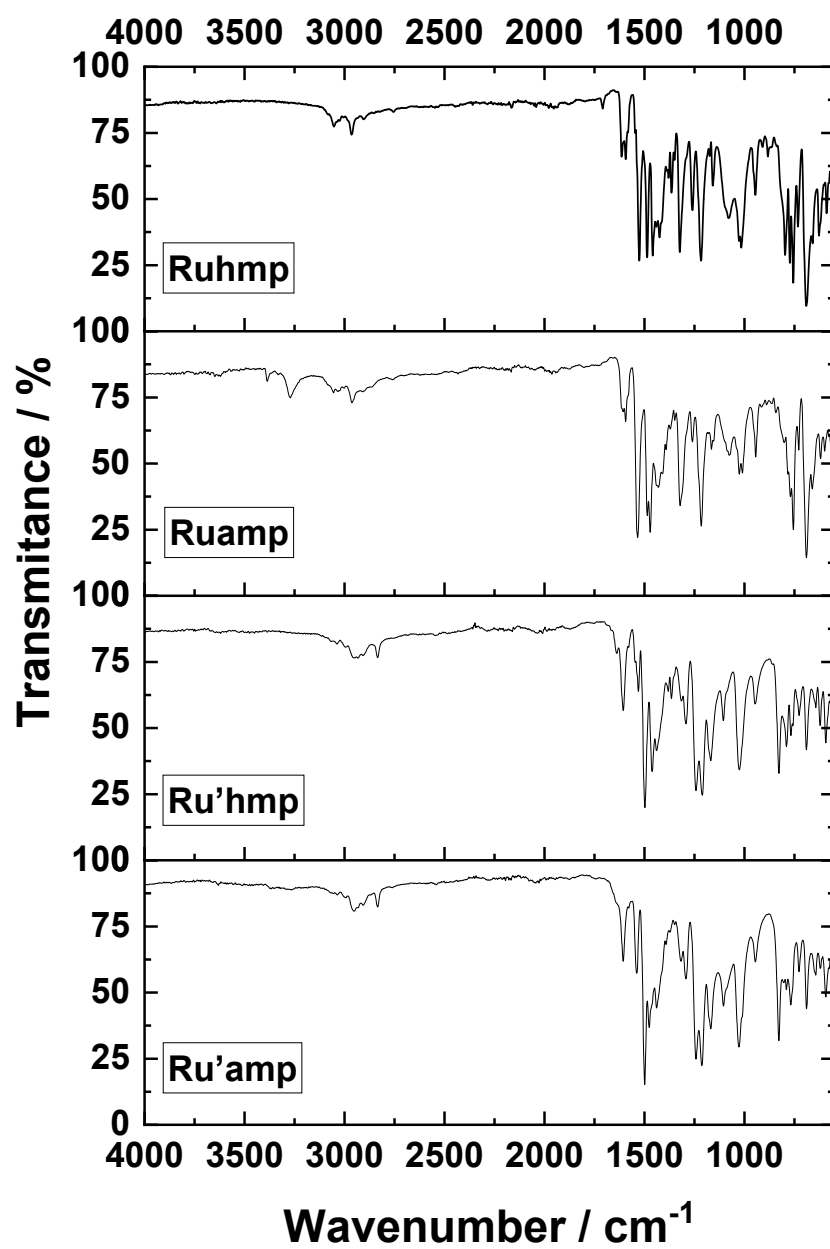


Figure S7. Infrared spectra of Ruhmp, Ruamp, Ru'hmp and Ru'amp.

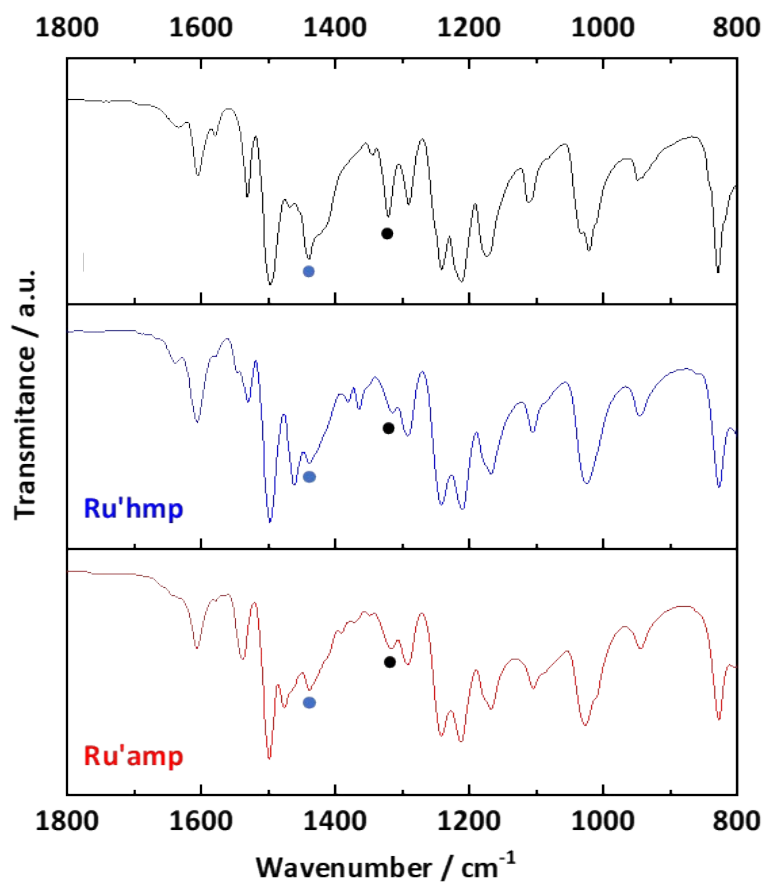


Figure S8. Comparison between the IR spectra of *cis*-[Ru₂Cl(μ-DAniF)₂(μ-OAc)₂] (black), **Ru'hmp** (blue) and **Ru'amp** (red). The O-C-O antisymmetric stretching bands are marked with blue circles and the symmetric ones with a black circle.

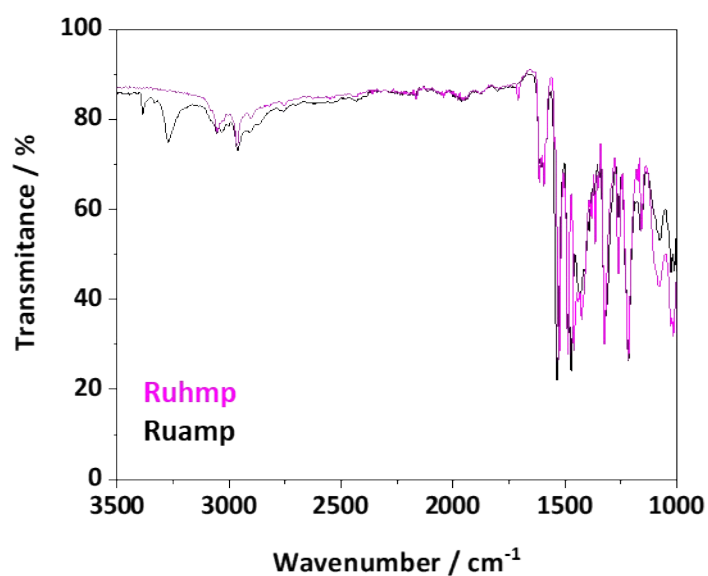


Figure S9. Comparison between the IR spectra of **Ruhmp** (pink) and **Ruamp** (black).

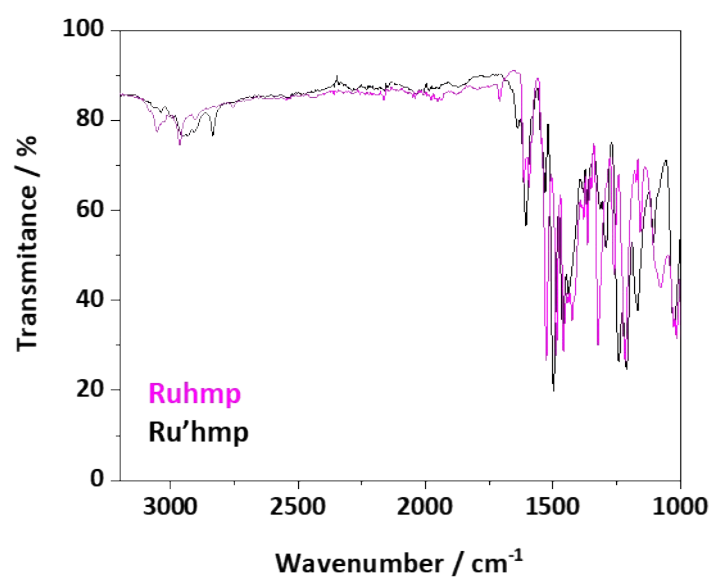


Figure S10. Comparison between the IR spectra of **Ruhmp** (pink) and **Ru'hmp** (black).

S3. Single crystal X-ray diffraction

Table S1. Crystal and structure refinement data for **Ruhmp**.

Empirical formula	C ₃₄ H ₃₁ ClN ₅ O ₃ Ru ₂
Formula weight	795.23
Temperature/K	100.0
Crystal system	monoclinic
Space group	<i>P</i> 2 ₁ / <i>n</i>
<i>a</i> /Å	9.8282(5)
<i>b</i> /Å	19.5453(9)
<i>c</i> /Å	16.2510(8)
α /°	90
β /°	98.094(2)
γ /°	90
Volume/Å ³	3090.6(3)
<i>Z</i>	4
$\rho_{\text{calc}}/\text{g}\cdot\text{cm}^{-3}$	1.709
μ/mm^{-1}	9.072
<i>F</i> (000)	1596.0
Crystal size/mm ³	0.208 × 0.049 × 0.03
Radiation	CuK α (λ = 1.54178)
2 θ range for data collection/°	7.116 to 136.482
Index ranges	-11 ≤ <i>h</i> ≤ 11, -23 ≤ <i>k</i> ≤ 23, -19 ≤ <i>l</i> ≤ 19
Reflections collected	91840
Independent reflections	5652 [<i>R</i> _{int} = 0.0718, <i>R</i> _{sigma} = 0.0261]
Data/restraints/parameters	5652/0/408
Goodness-of-fit on <i>F</i> ²	1.073
Final <i>R</i> indexes [<i>I</i> ≥ 2 σ (<i>I</i>)]	<i>R</i> ₁ = 0.0357, <i>wR</i> ₂ = 0.1003
Final <i>R</i> indexes [all data]	<i>R</i> ₁ = 0.0373, <i>wR</i> ₂ = 0.1018
Largest diff. peak/hole / e ⁻ Å ⁻³	1.56/-0.89

Table S2. Crystal and structure refinement data for **Ruamp**·Et₂O.

Empirical formula	C ₃₈ H ₄₂ ClN ₆ O ₃ Ru ₂
Formula weight	868.36
Temperature/K	100.0
Crystal system	monoclinic
Space group	<i>P</i> 2 ₁ / <i>n</i>
<i>a</i> /Å	12.6609(6)
<i>b</i> /Å	12.1468(6)
<i>c</i> /Å	24.3520(12)
α /°	90
β /°	100.814(2)
γ /°	90
Volume/Å ³	3678.6(3)
<i>Z</i>	4
$\rho_{\text{calc}}/\text{g}\cdot\text{cm}^{-3}$	1.568
μ/mm^{-1}	7.681
<i>F</i> (000)	1764.0
Crystal size/mm ³	0.284 × 0.045 × 0.016
Radiation	CuK α (λ = 1.54178)
2 θ range for data collection/°	7.37 to 136.49
Index ranges	-15 ≤ <i>h</i> ≤ 15, -14 ≤ <i>k</i> ≤ 14, -29 ≤ <i>l</i> ≤ 29
Reflections collected	115688
Independent reflections	6738 [<i>R</i> _{int} = 0.0634, <i>R</i> _{sigma} = 0.0222]
Data/restraints/parameters	6738/0/459
Goodness-of-fit on <i>F</i> ²	1.070
Final <i>R</i> indexes [<i>I</i> ≥ 2 σ (<i>I</i>)]	<i>R</i> ₁ = 0.0264, <i>wR</i> ₂ = 0.0749
Final <i>R</i> indexes [all data]	<i>R</i> ₁ = 0.0272, <i>wR</i> ₂ = 0.0756
Largest diff. peak/hole / e·Å ⁻³	0.67/-0.90

Table S3. Crystal and structure refinement data for **Ru'hmp**.

Empirical formula	C ₃₈ H ₃₉ ClN ₅ O ₇ Ru ₂
Formula weight	915.33
Temperature/K	100.0
Crystal system	monoclinic
Space group	<i>P</i> 2 ₁ / <i>n</i>
<i>a</i> /Å	12.5721(7)
<i>b</i> /Å	21.1723(9)
<i>c</i> /Å	13.9407(7)
α /°	90
β /°	97.231(4)
γ /°	90
Volume/Å ³	3681.2(3)
<i>Z</i>	4
$\rho_{\text{calc}}/\text{g}\cdot\text{cm}^{-3}$	1.652
μ/mm^{-1}	7.788
<i>F</i> (000)	1852.0
Crystal size/mm ³	0.064 × 0.044 × 0.021
Radiation	CuK α (λ = 1.54178)
2 θ range for data collection/°	7.636 to 136.48
Index ranges	-15 ≤ <i>h</i> ≤ 14, -25 ≤ <i>k</i> ≤ 24, -16 ≤ <i>l</i> ≤ 16
Reflections collected	88199
Independent reflections	6684 [<i>R</i> _{int} = 0.1964, <i>R</i> _{sigma} = 0.0805]
Data/restraints/parameters	6684/0/484
Goodness-of-fit on <i>F</i> ²	1.025
Final <i>R</i> indexes [<i>I</i> ≥ 2 σ (<i>I</i>)]	<i>R</i> ₁ = 0.0687, <i>wR</i> ₂ = 0.1593
Final <i>R</i> indexes [all data]	<i>R</i> ₁ = 0.1250, <i>wR</i> ₂ = 0.1914
Largest diff. peak/hole / e \cdot Å ⁻³	0.99/-1.54

Table S4. Crystal and structure refinement data for **Ru'amp·0.5C₆H₁₂**.

Empirical formula	C ₄₁ H ₄₆ ClN ₆ O ₆ Ru ₂
Formula weight	956.43
Temperature/K	150.00(10)
Crystal system	triclinic
Space group	<i>P</i> -1
<i>a</i> /Å	12.9823(4)
<i>b</i> /Å	13.7386(4)
<i>c</i> /Å	14.3812(4)
α /°	93.766(2)
β /°	109.216(3)
γ /°	112.885(3)
Volume/Å ³	2175.45(12)
<i>Z</i>	2
$\rho_{\text{calc}}/\text{g}\cdot\text{cm}^{-3}$	1.460
μ/mm^{-1}	6.603
<i>F</i> (000)	974.0
Crystal size/mm ³	0.146 × 0.079 × 0.069
Radiation	CuK α (λ = 1.54184)
2 θ range for data collection/°	6.676 to 154.144
Index ranges	-16 ≤ <i>h</i> ≤ 16, -17 ≤ <i>k</i> ≤ 17, -16 ≤ <i>l</i> ≤ 18
Reflections collected	25322
Independent reflections	8721 [<i>R</i> _{int} = 0.0151, <i>R</i> _{sigma} = 0.0157]
Data/restraints/parameters	8721/0/626
Goodness-of-fit on <i>F</i> ²	1.094
Final <i>R</i> indexes [<i>I</i> ≥ 2 σ (<i>I</i>)]	<i>R</i> ₁ = 0.0352, <i>wR</i> ₂ = 0.1165
Final <i>R</i> indexes [all data]	<i>R</i> ₁ = 0.0366, <i>wR</i> ₂ = 0.1177
Largest diff. peak/hole / e·Å ⁻³	1.33/-0.70

S4. Magnetic measurements

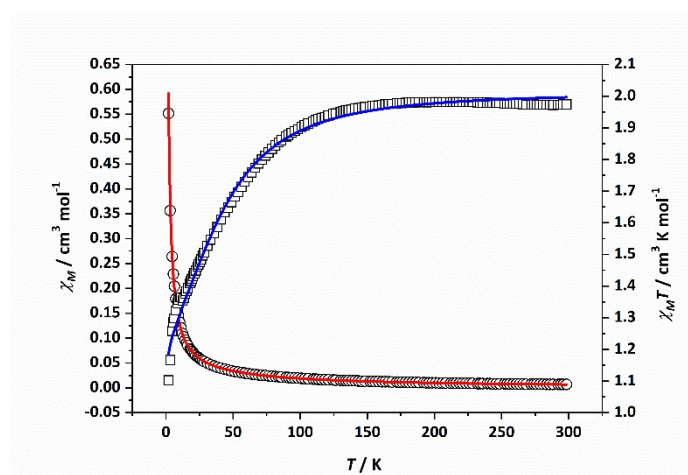


Figure S11. Temperature dependence of the molar susceptibility χ_M (circles) and $\chi_M T$ (squares) for **Ru'hmp**. Solid lines are the best fit to the data as described in the text.

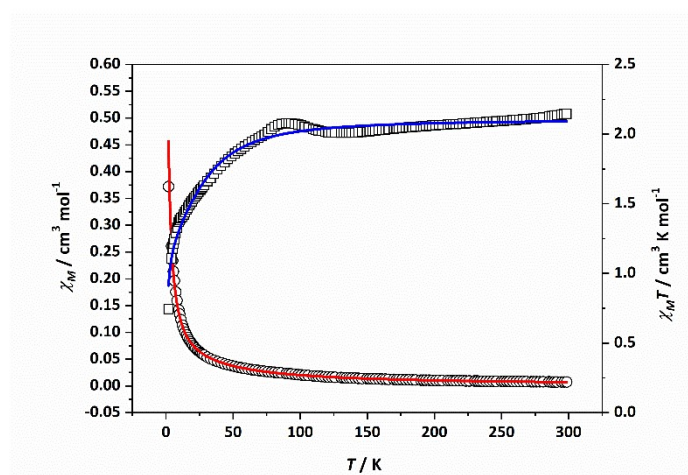


Figure S12. Temperature dependence of the molar susceptibility χ_M (circles) and $\chi_M T$ (squares) for **Ru'amp**. Solid lines are the best fit to the data as described in the text.

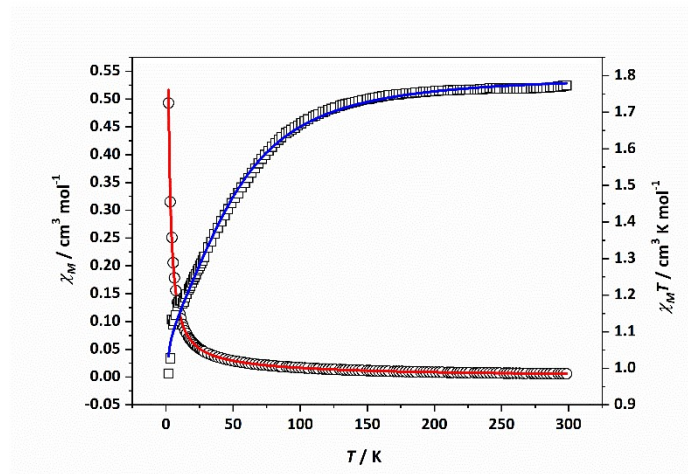


Figure S14. Temperature dependence of the molar susceptibility χ_M (circles) and $\chi_M T$ (squares) for **Ru'amp**. Solid lines are the best fit to the data as described in the text.

Equations S1-S4 employed in the fitting of the magnetic data:

$$\chi_M = \frac{\chi_{\parallel} + 2\chi_{\perp}}{3}$$

Equation S1

$$\chi_{\parallel} = \left(\frac{Ng^2\beta^2}{k_B T} \right) \left[\frac{1 + 9\exp\left(-2D/k_B T\right)}{4\left(1 + \exp\left(-2D/k_B T\right)\right)} \right]$$

Equation S2

$$\chi_{\perp} = \left(\frac{Ng^2\beta^2}{k_B T} \right) \left[\frac{4 + \left(\frac{3k_B T}{D}\right)\left(1 - \exp\left(-2D/k_B T\right)\right)}{4\left(1 + \exp\left(-2D/k_B T\right)\right)} \right]$$

Equation S3

$$\chi_M' = \frac{\chi_M}{1 - \left(\frac{2zJ}{Ng^2\beta^2}\right)\chi_M}$$

Equation S4

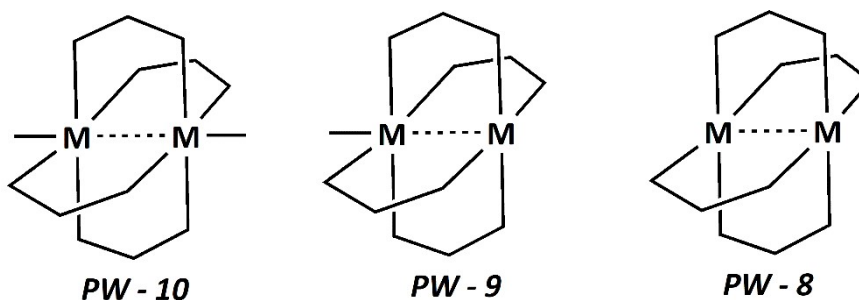
(N , g , β , and k_B have their usual meanings)

S5. Procedure employed to assign polyhedral symbol, coordination index, configuration number and chirality symbol to coordination compounds with paddlewheel structure

In order to fully describe the configuration of a coordination compound, three factors have to be provided:¹ the coordination geometry (overall shape of the molecule), the relative configuration (relative position of the components) and the absolute configuration (specific enantiomer when the mirror images are non-superimposable).

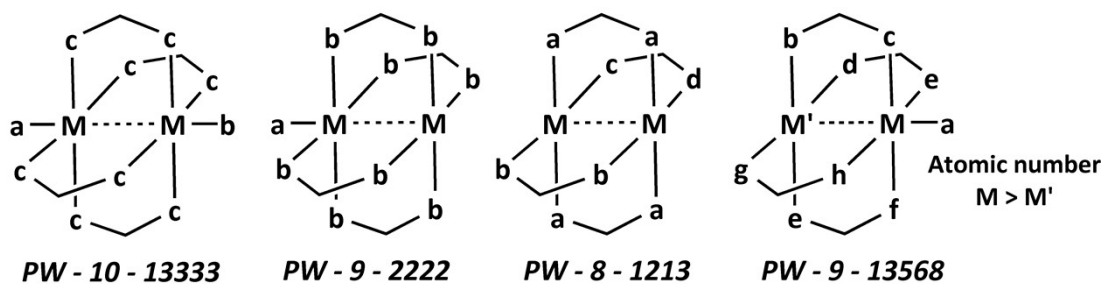
Coordination geometry

Binuclear paddlewheel compounds are characterized by the presence of two metal centers, usually bonded, and four bridging ligands between them. In addition, they can have two, one or no donor atoms at the axial positions. The chosen polyhedral symbol for these complexes is *PW* followed by the coordination number: 10, 9 or 8, respectively:



Configuration number

This number allows the distinction among the different possible isomers. To obtain it, a priority number based on Cahn–Ingold–Prelog rules² is assigned to the donor atoms of the ligands. Then, a number associated to each metal center is obtained starting by the axial position (if occupied) followed by the other four equatorial positions searching the lowest number possible. When the metal centers are not the same, the number selected for the configuration number is the one obtained from the metal center with highest atomic number (or atomic mass if they are isotopes). When both metal centers are equal, the metal with the lowest number is selected to define the configuration number. Different examples of the number assignment are depicted below.



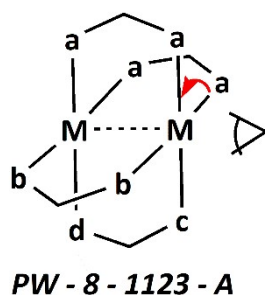
Absolute configuration: chirality symbol

The chirality symbol is obtained from the configuration number following the sequence from the highest to the lowest priority number considering the point of view from outside of the chosen metal center. If the sequence proceeds in a clockwise fashion, it is assigned the chirality symbol *C*; if the sequence proceeds anticlockwise, it is assigned *A* as

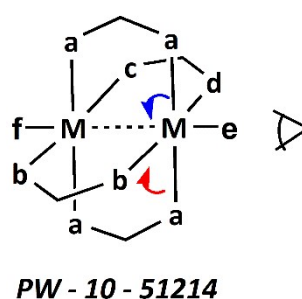
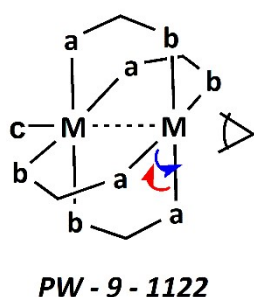
¹ Nomenclature of Inorganic Chemistry. IUPAC Recommendations 2005; N. G. Connelly, Royal Society of Chemistry (Great Britain), International Union of Pure and Applied Chemistry, Eds.; Royal Society of Chemistry Publishing/IUPAC: Cambridge, UK, (2005).

² (a) R. S. Cahn, C. Ingold, V. Prelog, Specification of Molecular Chirality. *Angew. Chem. Int. Ed. Engl.*, 1996, **5** (4), 385–415. (b) V. Prelog, G. Helmchen, G. Basic Principles of the CIP-System and Proposals for a Revision. *Angew. Chem. Int. Ed. Engl.*, 1982, **21** (8), 567–583.

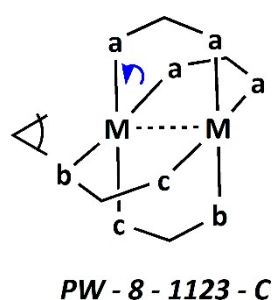
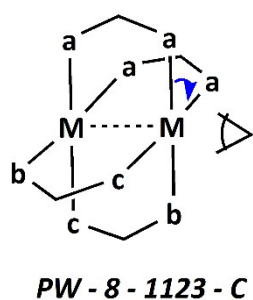
chirality symbol. These symbols are selected because the chirality arises from the distribution of the donor atoms/ligands around the stereogenic metal-metal bond.



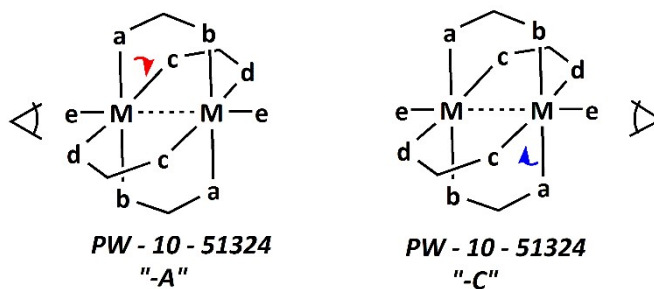
If the sequence can go both clockwise and anticlockwise, the complex is not chiral:



When the two sequence numbers are equal, the two sequences must be checked to get the chirality symbol. If both provide the same symbol, the complex is chiral;



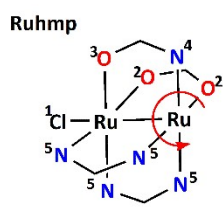
if they provide different chirality symbols, the compound is not chiral:



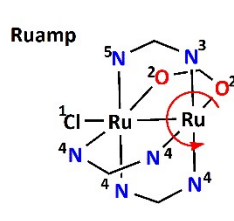
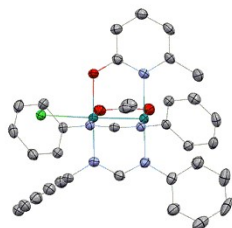
There is an inversion center.

In this case, and if both metals are equal, there is an inversion center placed between the two metal atoms. If the metals are different, the chirality index is assigned using the metal with the lowest configuration number. If both are equal, the heaviest metal is chosen.

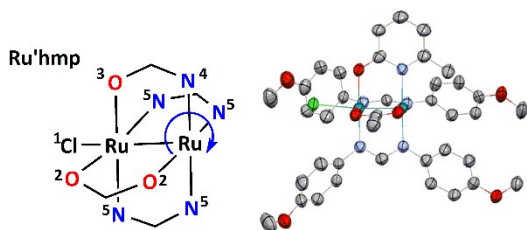
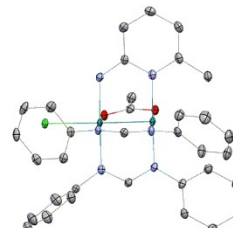
Following the procedure herein described, the polyhedral symbol, coordination index, configuration number and chirality symbol of the molecules found in the asymmetric unit of the centrosymmetric crystal structures of **Ruhmp**, **Ruamp**, **Ru'hmp**, and **Ru'amp** are *PW-9-2455-A*, *PW-9-2344-A*, *PW-9-2455-C*, and *PW-9-2344-C*, respectively (see below).



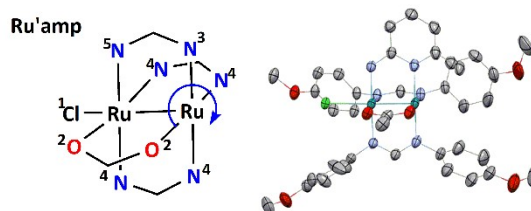
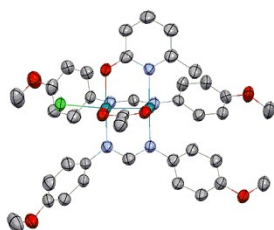
PW-9-2455-A



PW-9-2344-A



PW-9-2455-C



PW-9-2344-C

